

About the Reliability of Particle in Cell Methods and the Notion of a “Local” Temperature of Ionized Species Around a Spacecraft in the Ionosphere

Roger Godard, and John D. de Boer

Department of Mathematics and Computer Science, RMCC, Kingston, Canada

Abstract: The development of space science has generated important computer codes for the simulation of the interaction between complex space structures (artificial satellites, solar panels, etc.) and the surrounding plasma. The basic equation to be solved is the Poisson equation for the electric potential around a structure. Here, we try to study analytically the shadowing effect of a spacecraft on an electrode for the electron number density and the electron temperature. We suggest that the electron temperature should be taken as a variable and not as a parameter. However, its computation involves the knowledge of the histogram of the distribution of the frequencies of the electron velocities inside the computational cells. Also, we have illustrated the possibilities of artefacts due to the design and geometry of scientific instruments for the measurement of the electron number density and the electron temperature in the ionosphere. We suggest an optimal design for an electrode and its guard ring.

Keywords: Plasma physics, particle-in-cell methods (PIC), electron number density, definition of the electron temperature.

1. Introduction

The development of space science has generated important computer codes for the simulation of the interaction between complex space structures (artificial satellites, solar panels, etc.) and the surrounding plasma [1-3]. For example, when a satellite moves through the ionosphere, it creates an electrostatic wake in the downstream region. This modifies the trajectories of the ionized species (ions and electrons) of a collisionless plasma and creates a perturbation of the data collected for scientific measurements in both the upstream and the downstream regions. The basic equation to be solved is the Poisson equation for the electric potential ϕ around the structure:

$$\nabla^2 \phi(\mathbf{r}) = -e(N_i(\mathbf{r}) - N_e(\mathbf{r})), \quad \phi < 0 \quad (1)$$

Where \mathbf{r} is the position vector, e the elementary charge, N_i the ion number density, and N_e the electron

number density. The densities are estimated by Particle-In-Cell methods (PIC methods), and this requires a large number of test particles. In the PIC methods, test particles are injected at random into the computational domain from the outer boundary and from a given distribution function of the velocities. For example, for the study of the Earth Magnetic Field Effects on Particle Sensors on LEO Satellites, the mesh consisted of 4400207 tetrahedral elements and a total of 500 million test particles [2]. In order to save computer time, and to decrease numerical noise, many researchers do not explicitly compute the density of repelled species, they utilize a hybrid Boltzmann-PIC code as follows [3, 4]:

$$\nabla^2 \phi(\mathbf{r}) = -e \left(N_i(\mathbf{r}) - N_{e,+\infty} \exp\left(\frac{e\phi(\mathbf{r})}{k_B T_e}\right) \right), \quad \phi < 0 \quad (2)$$

Here, $N_{e,+\infty} = \lim_{r \rightarrow +\infty} N_e(\mathbf{r})$ is the ambient electron density, k_B is the Boltzmann constant, and T_e is the electron temperature which is assumed to be a

Corresponding author: John D. de Boer, Assistant Professor, research field: plasma physics, numerical methods, unstructured meshes. E-mail: pthroughz@gmail.com.

parameter. $N_{e,+\infty} \exp\left(\frac{e\phi(\mathbf{r})}{k_B T_e}\right)$ is called the

Boltzmann factor. A minor improvement, in the presence of a wall, would be to introduce a “weight” function $w(\mathbf{r})$ such as:

$$N_e(\mathbf{r}) = w(\mathbf{r}) \times \frac{N_{e,+\infty}}{2} \exp\left(\frac{e\phi(\mathbf{r})}{k_B T_e}\right); \quad (3)$$

$$w(\mathbf{r} \rightarrow +\infty) = 2; \quad w(\mathbf{r} = \mathbf{r}_s) = 1.$$

Where \mathbf{r}_s represents one point at the surface of a structure. Eq. 3 takes into account the fact that a wall introduces a screening effect on the number density at the surface of an object.

We want to illustrate that the physics is more complex than in Eq. 3, and in this work we shall consider the temperatures of the ionized species not as parameters but variables as functions of \mathbf{r} , just like the number densities of the charged species in the vicinity of a structure (electrode or satellite). A few codes perform a full PIC simulation of both ions and electrons; for example, the Democritus code was written for an axially symmetric flow for a collisionless, magnetized plasma for the study of

tokamaks [4, 5]. The codes were written in the limit of a vanishing Debye length. Also, the interaction between the space plasma and an artificial satellite has attracted theoreticians and numerical analysts. In the code PTetra [2], plasma species are treated fully kinetically with PIC models. The advance in computer codes and the fact that particle pushers are highly parallelizable have made complex Poisson solvers possible.

2. Early Rocket Experiments

Early rocket experiments have brought out spin and coning effects on the measurements of the electron temperature in the ionosphere from electrostatic (Langmuir) and electromagnetic probes on board a payload [6]. For example, Fig. 1 showed the effect of rocket roll on (A) the electron temperature, and (B), the electron number density on an earlier rocket experiment of the French National Center of Space Studies. The electron temperature illustrated an apparent increase in the electrostatic wake and also the electron number density showed a decrease. The instruments were mounted at the extremities of two opposite booms.

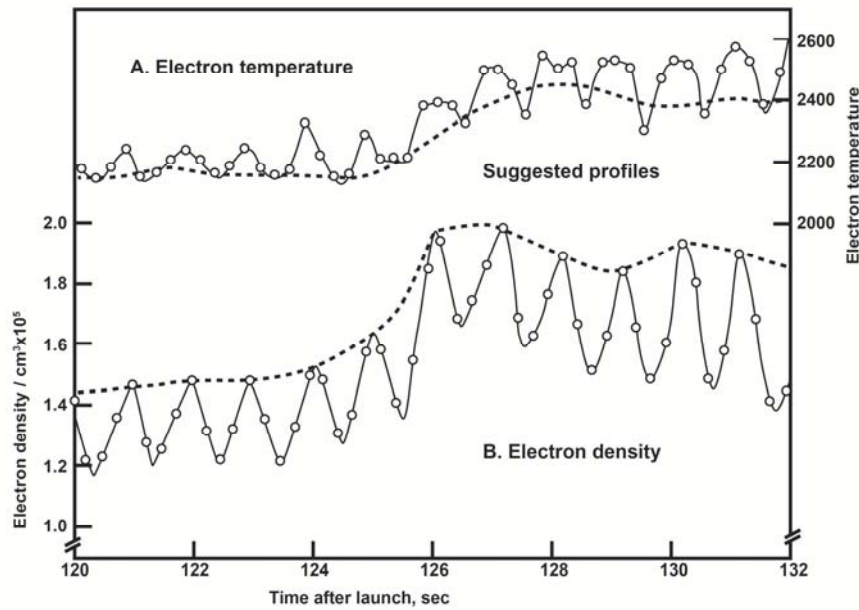


Fig. 1 The effect of rocket roll on the electron temperature and the electron number density [6].

Experimenters did not have a full explanation for these phenomena. Here, we shall assume that the electron temperature is a function of the position vector \mathbf{r} , and the direction and magnitude of the drift velocity \mathbf{U} of a payload. We shall write the electron temperature as $T_e(\mathbf{r})$. The ambient electron temperature will be defined as $T_e = T_{e,+\infty} = \lim_{\mathbf{r} \rightarrow +\infty} T_e(\mathbf{r})$.

3. The Definition of the Local Temperatures for Ionized Species

Wu [7] defines the temperature of neutral species by the following integral equation:

$$N_n \frac{3}{2} k_B T_n = \int \frac{1}{2} m_n v^2 f(\mathbf{r}, \mathbf{v}, t) d^3 \mathbf{v} \quad (4)$$

where N_n is the number density for neutral particles,

T_n their temperature, $\frac{3}{2}$ is a factor of normalization,

m_n is their mass, $f(\mathbf{r}, \mathbf{v}, t)$ the distribution function which is defined by a position vector \mathbf{r} , a velocity vector \mathbf{v} , and the time t . Therefore, it seems normal to link the temperature to the kinetic energy. Eq. (4) indicates that if the distribution function is Maxwellian, we have equilibrium. In this work, we define the temperature of neutrals in spherical coordinates by the expectation of the kinetic energy as follows:

$$N_n \frac{3}{2} k_B T_n = N_n \left(\frac{m_n}{2\pi k_B T_n} \right)^{3/2} \int_0^{+\infty} \frac{1}{2} m_n v^2 \exp\left(-\frac{m_n v^2}{2k_B T_n}\right) 4\pi v^2 dv \quad (5)$$

Very rarely, the temperature of ionized species is defined in plasma physics. Generally, and by analogy with the neutrals, the temperature is taken as a constant parameter, but this does not fully explain the anomalies that we observe experimentally. In their computer code SCEPTIC3D, Patacchini and

Hutchinson [5] defined an ion temperature by a covariance around a sphere and for a highly anisotropic medium. Here they assumed a constant electron temperature. In the code UPIC3dE, Gatsonis and Spirkin [1] defined mass-average temperatures for different species T_s^* by an expectation:

$$\frac{3}{2} k_B T_s^*(\mathbf{r}, t) = \frac{1}{2} m \langle v_s^{(*)2} \rangle. \quad (6)$$

The subscript s identifies the species.

4. The Case of a Potential Well: A Hypothesis

For simplicity, we shall consider the case of an electric potential well with no wall effects [8]. We shall develop formulas for repelled species only, i.e., electrons for a negative potential well $\phi(r)$. Let us consider particles of mass m and charge q (either ions or electrons) immersed in a three-dimensional potential well. Let us consider particles coming from infinity. Far from the well, ionized particles have a

kinetic energy $E = \frac{1}{2} m v(\mathbf{r} \rightarrow +\infty)^2$. These

particles can reach a point \mathbf{r} of the well, if at this

point, $E(\mathbf{r}) = q\phi(\mathbf{r}) + \frac{1}{2} m v(\mathbf{r})^2 > 0$. For

attracted ionized species, the lower bound of integration for the velocity is

$v(\mathbf{r}) > [-2q\phi(\mathbf{r})/m]^{1/2}$. For repelled ionized

species, we must take as the lower bound of integration, $v(\mathbf{r}) > 0$. For all repelled species,

including electrons in a negative potential well, we can apply the same definition that the one for neutrals at a point \mathbf{r} , and obtain :

$$N_{e,+\infty} \frac{3}{2} k_B T_e(\mathbf{r}) \exp\left(\frac{e\phi(\mathbf{r})}{kT_e}\right) = N_{e,+\infty} \left(\frac{m_e}{2\pi k_B T_e}\right)^{3/2} \exp\left(\frac{e\phi(\mathbf{r})}{kT_e}\right) \int_0^{+\infty} \frac{1}{2} m_e v^2 \exp\left(-\frac{m_e v^2}{2k_B T_e}\right) 4\pi v^2 dv. \quad (7)$$

If $\phi(\mathbf{r} \rightarrow +\infty) = 0$, we obtain the same relation as the one for neutral species. For attracted species, the formula is more complicated because of the lower bound of integration. We need to compute numerically the right-hand side of (7) by estimating the histogram $h(v)$ of the distribution of frequencies for velocities. We have:

$$N_{e,+\infty} \frac{3}{2} k_B T_e(\mathbf{r}) = \sum \frac{1}{2} m_e v^2 h(v) 4\pi v^2 \Delta v \quad (8)$$

Note that $h(v)$ is not the true distribution function. In the ionosphere, the distribution functions for ions and electrons are rarely Maxwellian, and if these distributions are available, it would be one way to estimate the temperatures. Moreover, Eqs. (7) and (8)

$$N_e(r) = N_{e,+\infty} \left(\frac{m_e}{2\pi k_B T_e} \right)^{3/2} \int_{E=q\phi}^{+\infty} \exp\left(-\frac{q\phi + 1/2 m_e v^2}{k_B T_e} \right) \xi(E) 4\pi v^2 dv \quad (9)$$

or more generally:

$$N_e(\mathbf{r}) \approx \exp\left(\frac{e\phi(\mathbf{r})}{k_B T_e} \right) \sum \tilde{h}(\mathbf{r}, \mathbf{v}, \phi) 4\pi v^2 \Delta v \quad (10)$$

Here, we take into account the shadowing effect, and a more complex distribution function than a Maxwellian one, in \tilde{h} . The situation is very complex

illustrate the limitations of the fluid models for the modeling of the ionosphere, because the temperatures are linked to the distribution functions. The presence of a conducting structure (electrode, satellite) will truncate the distribution function, and it introduces a shadowing effect, and a particle removal. Fig. 2 shows the interaction between a spherical spacecraft and an electrode mounted at the extremity of a boom.

In 1974, Laframboise and Godard computed the populated fraction $\xi(E)$ of orbits at a point of interest, in the vicinity of a spherical spacecraft [9]. Here, E is the total energy. They integrated over the velocity space to obtain the total density reduction at a point \mathbf{r} in the space. For a repelling spacecraft, we have:

for 3D spacecraft. Indeed, scientists do not compute the electron number density from Eq. 10. They just count the number of test particles in a computational cell, and then they normalize this number with respect to the ambient number density. We can generalize Eq. 9 to the definition of the temperatures for ionized species. For example, for a repelling spacecraft:

$$N_{e,+\infty} \frac{3}{2} k_B T_e(r) \exp\left(\frac{e\phi}{k_B T_e} \right) \approx N_{e,+\infty} \left(\frac{m_e}{2\pi k_B T_e} \right)^{3/2} \int_{E=-e\phi}^{+\infty} \frac{1}{2} m_e v^2 \exp\left(-\frac{-e\phi + 1/2 m_e v^2}{k_B T_e} \right) \xi(E) 4\pi v^2 dv \quad (11)$$

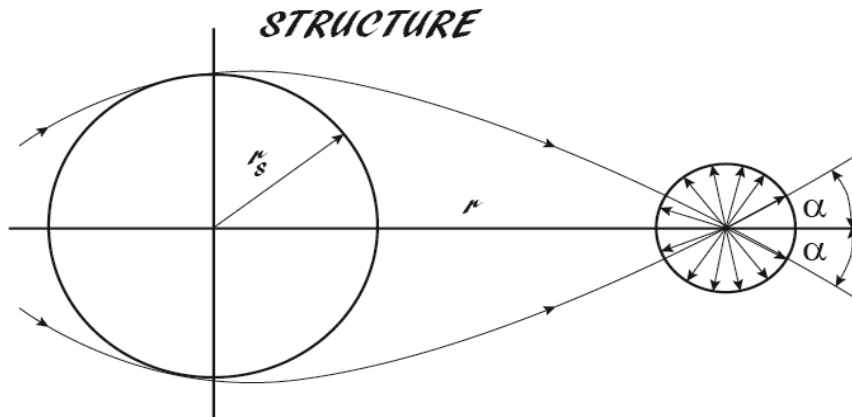


Fig. 2 The figure represents the interaction between a spherical structure and an electrode mounted at the extremity of a boom. We see the cut-off angle 2α for particle orbits all corresponding to the same total energy at the electrode location.

In such case, this will be the definition of a local electron temperature at the position r . Eq. (11) explains that the presence of a structure modifies the local temperature in its vicinity. If the distribution is not Maxwellian, and if we take into account the shadowing effect, we shall obtain:

$$N_{e,+\infty} \frac{3}{2} k_B T_e(\mathbf{r}) \approx \sum \frac{1}{2} m_e v^2 \tilde{h}(\mathbf{r}, \mathbf{v}, \phi) 4\pi v^2 \Delta v \quad (12)$$

The PIC methods automatically take into account the shadowing effect of a spacecraft, and particle removals, but the Boltzmann factor does not. Note that Eq. (12) does not imply a modification of the Vlasov equation. This last equation states that the distribution function stays constant along a trajectory in the phase plane [10]. Here, \tilde{h} implies that we have a sink of particles or an artificial perturbation of the electron temperature at the point \mathbf{r} . More specifically, scientific instruments are mounted at the extremity of a boom, away from the body of a spacecraft. Then, Eq. (12) implies that:

$$T_e(a) = T_e(\phi(\mathbf{r}_s), \phi(a), a). \quad (13)$$

Here a is, for example, the radius of a spherical electrode. We suggest adjusting the Boltzmann factor by:

$$N_e(\mathbf{r}) = N_{e,+\infty} \exp\left(\frac{e\phi(\mathbf{r})}{k_B T_e}\right) K(\phi(\mathbf{r}_s), \phi(a), \mathbf{r}), \quad \phi < 0 \quad (14)$$

where $K \leq 1$ is not a constant.

Let us re-examine the definition of the repelled electron flux collected by a spherical electrode from Laframboise and Parker in 1973 [8], but here we also include the shadowing effect of a structure. They used spherical coordinates (v, θ, ψ) in the velocity space, with polar axis in the x direction so that the flux I is given by:

$$I = \int_{E=q\phi}^{+\infty} f v_x \xi(E) d^3 \mathbf{v}. \quad (15)$$

Eq. (15) does not possess an analytical solution,

except in the case where $\xi(E) = 1$, i.e., if we have no shadowing effect, we obtain the classical result of the electron flux for a negative potential [12, 15]:

$$I_e = \frac{1}{4} N_{e,+\infty} e \sqrt{\frac{8k_B T_e}{\pi m_e}} \exp\left[\frac{e\phi}{k_B T_e}\right]; \quad \phi < 0. \quad (16)$$

It is difficult to estimate the shadowing effect or a wake effect on the flux. $\xi(E)$ is a non-linear function of the potential of the electrode. For example, if $\xi(E)$ is weaker near the plasma potential than expected, this will translate to an apparently higher measured electron temperature by a Langmuir probe,

5. Applications to Data Processing of the Earlier Rocket Experiment

In Fig. 1B, the electron density profile was obtained directly from an impedance probe, also called a Sayers probe. Two small grid-like electrodes formed a capacitor at a probing frequency of 39 MHz. The measured capacitance between the electrodes was proportional to the electron number density [6, 13, 14]. This impedance probe was therefore an electromagnetic instrument. It is easy to explain the strong payload roll effect because of a bad separation between the rocket and the payload. Because the payload had a larger drift velocity \mathbf{U} than the ion velocity $\sqrt{2k_B T_i / m_i}$, they had formation of an electrostatic wake in the downstream region. Here, the subscript i refers to the ions, T_i is the ion temperature, and m_i the average ion mass. Note that, as McMahon [11] said, "The ion number density field in the wake of a structure has a complicated behaviour which is strongly dependent upon the drift velocity \mathbf{U} ", the plasma parameters, and the geometry of a structure. Scientists divide the wake into three regions: the near wake where the ion depletion may be important; the mid wake, where enhanced ion number densities may exist because of a focusing effect of ion trajectories; and finally the last region is called the far wake. Because electrons and ions are linked through

the Poisson equation, the electron number density is also affected in the wake region. However, our Eq. (14) shows that even in the upstream region, we may have a shadowing effect and a depletion of the electron number density. Also, in the upstream region, measurements can be affected by encircling trajectories around the structure. It is most unfortunate that modellers studied in depth only the behaviour of the ion number density in the electrostatic wake, and not the electron number density. It would be interesting to know the behaviour of the electron number density in the near wake, the mid wake, and the far wake.

Note that for this particular rocket experiment, and in Fig. 1A, we observed an increase of the electron temperature in the wake region. At this stage, we must distinguish two different situations: the local temperature which is defined by Eq. (12), and an *estimation* of the electron temperature from an instrument on board and its collected current (Eq. (15)). We believe that we can explain the roll effect and the data presented on Fig. 1 with our model, if we accept that the population of occupied orbits is not the same in the upstream region and the downstream region (the wake) at the position of the instrument. There is one possibility that they had an artefact due to the geometry and the design of the instrument. The electron temperature sensor was a Sayers-Langmuir probe [8, 12, 15]. A Langmuir probe is an electrostatic instrument where an electrode is biased in potential, and the collected electron current enables the estimation of the electron temperature. We are going to split the interaction between a moving spacecraft and the ionosphere into two types of effect: a global effect, and a local effect in the vicinity of the instrument. The global effect includes the spacecraft, a boom, and an instrument mounted at the extremity of the boom, while the local effect is linked to the geometry and the design of the instrument. In this present work, we can only study the local effect because the global effect requires the knowledge of

the velocity of the payload and the attitude that we don't have. It would be also a complex full 3D simulation process.

In the Sayers-Langmuir electron temperature sensor [6], the apparatus consisted of two spherical electrodes, slightly differently biased in potential. These electrodes were separated from a cylindrical guard ring by an insulator of Teflon. Our purpose is to study the behaviour of the electric potential near the electrodes. Fig. 3 represents our computational grid. For simplicity, we have put a Neumann condition on the potential on the left side of the grid, a Neumann condition at the bottom of the grid, and two Dirichlet conditions on the other sides of the grid. They had a little rectangular electronic box at the end of the guard rings. However, we have artificially rounded the corners of the box in our grid structure for computational purposes. Also we have biased the electrode to a weak potential of -0.1 volt, the insulator to a potential of -1 volt, the guard ring at a potential of -0.1 volt, and the electronic box at a potential of -1 volt. The insulator is at a floating potential, i.e., the net collected current is zero. We assumed that the value of -1 volt was reasonable for the floating potential. This potential must be negative so that positive ions are attracted and the electrons are repelled.

Fig. 4 represents the contour map of the potential around the instruments. We observe potential barriers in the vicinity of the insulator. These barriers will prevent the collection of small energy electrons by the electrode. Consequently, they will correspond to a weaker electron current near the potential zero, which is also called the plasma potential. *This will translate to an apparent higher electron temperature.* Note also that the vicinity of the insulator corresponds to a concave region, and this may affect the collection of charged species. Now it is also possible that the ion and electron currents collected by the insulator were different in the upstream and downstream regions. This would affect the electron temperature measurements.

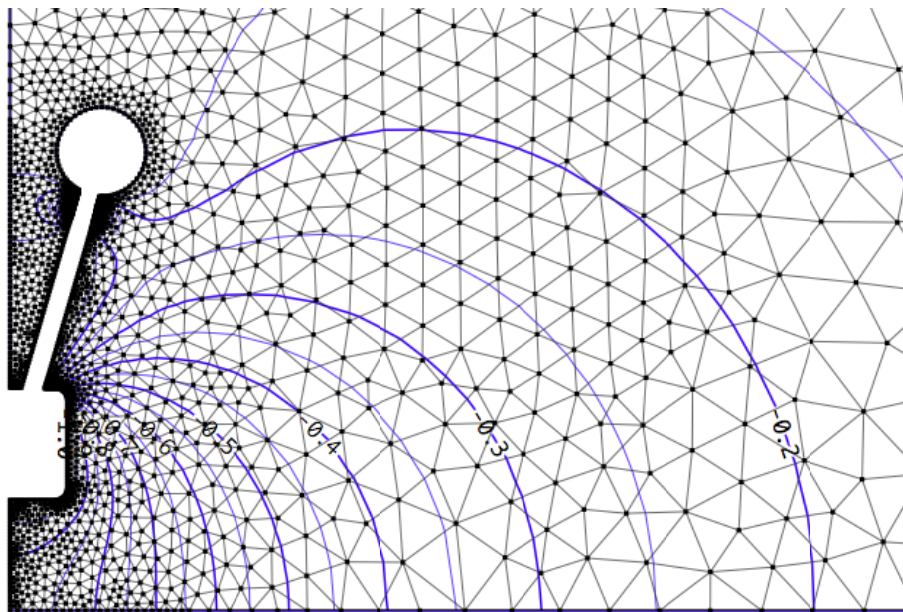


Fig. 3 The computational grid around one electrode for the design of the Sayers-Langmuir electron temperature probe.

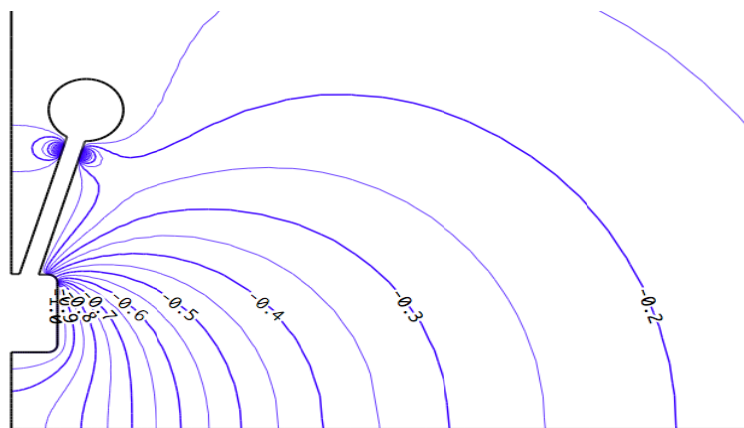


Fig. 4 Contour map of the potential around one electrode of the Sayers-Langmuir probe.

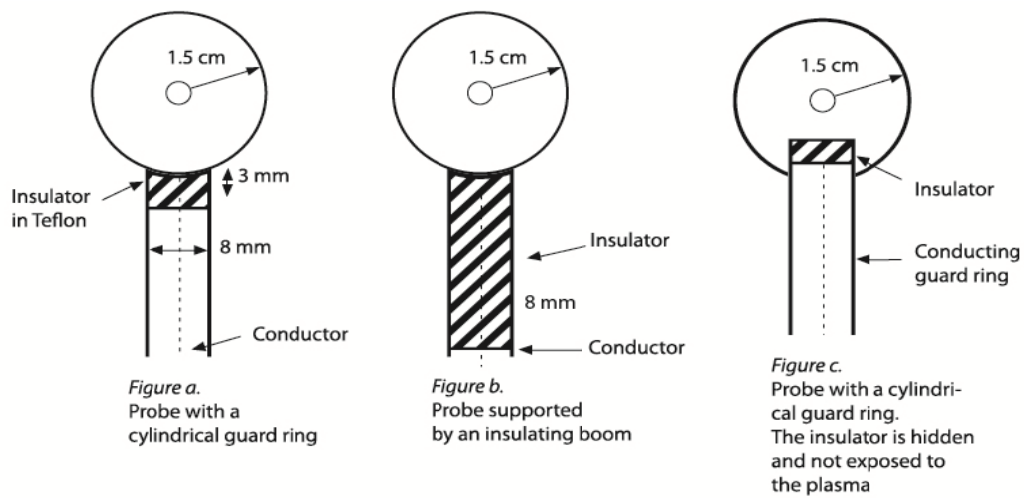


Fig. 5 New design of an electrode.

These perturbing effects of an isolator have inspired us to propose new designs of an electrode where the insulators are hidden [16].

Finally, we should emphasize that our definition of the local electron temperature differs from a temperature measured with a scientific instrument. This instrument may be subject to all types of anomalies, and perturbations.

6. Conclusion: Numerical Verifications of our Hypothesis about the Local Electron Temperature

For a very long time, the Boltzmann factor has been utilized by modelers for the solution of the Poisson equation. It is a convenient formula, easy to implement, and it has some smoothing properties for numerical solution of the Poisson equation. It may work well for a one-body problem, or it may be used as a guess field for full PIC simulation processes. For example, McMahon's PIC-Boltzmann code for the study of the interaction of infinite and finite cylindrical electrodes with a drifting collisionless Maxwellian plasma [11] fitted well with Laframboise's exact numerical results of a plasma at rest [12]. But these codes don't enable us to compute a contour map of the electron temperature around a body. Indeed, the case of a multi-body problem is more difficult. It will be computer time consuming to accurately compute the cut-off orbits. However, fully PIC codes would enable us to compute a map of the electron temperature and the electron number density around a complex structure. This would enable us to improve the design of space experiments, and provide better data processing. The computation of Eq. (12) would require 50 to 100 particles per populated cell in order to build an accurate histogram. The computation of the orbits for repelled species requires skill, and control of the total energy. For example, we must avoid shooting test particles directly at a structure, because the equations of motion for repelled species may not be defined at a turning point.

Acknowledgments

One author (RG) would like to thank J. J. Berthelier and J. J. Laframboise for very stimulating ideas.

References

- [1] Gatsonis, N. A. and Spirkin, A. (2009). “A Three-Dimensional Electrostatic Particle-In-Cell Methodology on Unstructured Delaunay-Voronoi Grids.” *J. Comp. Phys.* 228: 3742-3761.
- [2] Rehman, S. Ur, Marchand, R., Berthelier, J. J., Onishi, T., and Burchill, J. (2013). “Earth Magnetic Field Effects on Particle Sensors on LEO Satellites.” *IEEE Trans. Plasma Sci.* 41 (12): 3402-3409.
- [3] Davis, V. A. et al. (2013). “Comparison of Low Earth Orbit Wake Current Collection Simulations Using Nascap-2k, SPIS, and MUSCAT Computer Codes.” *IEEE Trans. Plasma Sci.* 41 (12): 3303-3309.
- [4] Patacchini, L. and Hutchison, I. H. (2007). “Electron Collection by a Negatively Charged Sphere in a Collisionless Magnetoplasma.” *Phys. Plasmas* 14: 062111-1.
- [5] Patacchini, L. and Hutchinson, I. H. (2010). “Spherical Probes at Ion Saturation in E×B Fields.” *Plasma. Phys. Control Fusion* 52: 035005.
- [6] Berthelier, J. J. and Sturges, D. (1967). “Simultaneous Measurements of Electron Density and Temperature in the Northern Auroral Zone.” *Planet. Space Sci.* 15: 1049-1054.
- [7] Wu, T. Y. (1966). *Kinetic Equations of Gases and Plasmas*, Addison-Wesley, Reading.
- [8] Laframboise, J. G. and Parker, L. W. (1973). “Probe Design for Orbit-Limited Current Collection.” *The Physics of Fluids* 16: 629-636.
- [9] Laframboise, J. G. and Godard, R. (1974). “Perturbation of an Electrostatic Probe by a Spacecraft at Small Speed Ratios.” *Planet. Space Sci.* 22: 1145-1155.
- [10] Godard, R. (2019). “Boltzmann and Vlasov, Research in History and Philosophy of Mathematics.” In: M. Zack, D. Schlim (Eds.), *Proceedings of 2017 CSHPM in Toronto*, Birkhäuser, New York, pp. 157-166.
- [11] McMahon, J. C. (2000). “The Interaction of Infinite and Finite Cylindrical Probes with a Drifting Collisionless Maxwellian Plasma.” Ph.D. thesis, York University, North York, Ontario, Canada.
- [12] Laframboise, J. G. (1966). “Theory of Spherical and Cylindrical Langmuir Probes in a Collisionless, Maxwellian Plasma at Rest.” UTIAS-University of Toronto, report No.100.
- [13] Sayers, J. (1970). “In Situ Probes for Ionospheric

Investigations.” *J. Atmos. Terrest. Phys.* 4: 663-691.

- [14] De Boer, J. and Godard, R. (1998). “Optimal Design of HF Impedance Probes.” In: *Proceedings of the 21st International Symposium on R.G.D.*, Marseille. Editor: R. Brun, Cépaduès-Éditions, France, Vol. 2, pp. 473-480.

- [15] Mott-Smith Jr. and Langmuir, I. (1926). “The Theory of

Collectors in Gaseous Discharges.” *Phys. Rev.* 28: 727-763.

- [16] Godard, R. (2005). *Some Examples of Optimal Design in Electrostatics and Electromagnetism: Boundary Elements XXVII*. WIT Press, pp. 663-673.